Micro-Scale Freeze-Drying with Raman Spectroscopy as a Tool for Process Development

SUPPORTING INFORMATION

ARI KAUPPINEN,[*,†] *MAUNU TOIVIAINEN,*[‡] *JAAKKO AALTONEN,*[§] *OSSI KORHONEN,*[†] *KRISTIINA JÄRVINEN,*[†] *MIKKO JUUTI,*[‡] *RIIKKA PELLINEN,*[‖] *JARKKO KETOLAINEN*[†]

[†]School of Pharmacy, Promis Centre, Faculty of Health Sciences, University of Eastern Finland, P.O. Box 1627, FI-70211 Kuopio, Finland

[‡]Optical Measurement Technologies, VTT Technical Research Centre of Finland, P.O. Box 1199, FI-70211 Kuopio, Finland

[§]Division of Pharmaceutical Technology, Faculty of Pharmacy, University of Helsinki, P.O. Box 56, FI-00014 Helsinki, Finland

[‖]A.I. Virtanen Institute for Molecular Sciences, Faculty of Health Sciences, University of Eastern Finland, P.O. Box 1627, FI-70211 Kuopio, Finland

Table of Contents

Table S-1. Freeze-drying process parameters of experiments A – D.

Process step	Experiment				Cryostage pressure (mTorr)
	A Fast cooling with annealing	B Fast cooling without annealing	C Standard cooling with annnealing	D Standard cooling without annealing	
Cooling					
+20°C → -50 °C	10 °C/min	10 °C/min	1 °C/min	1 °C/min	760000
Annealing					
-10 °C	5 min	-	5 min	-	760000
Primary drying					
-15 °C	30 min	30 min	30 min	30 min	55
Secondary drying					
+30 °C	10 min	10 min	10 min	10 min	
+60 °C	15 min	15 min	15 min	15 min	55
+80 °C	10 min	10 min	10 min	10 min	
Total process time	131 min	113 min	167 min	149 min	

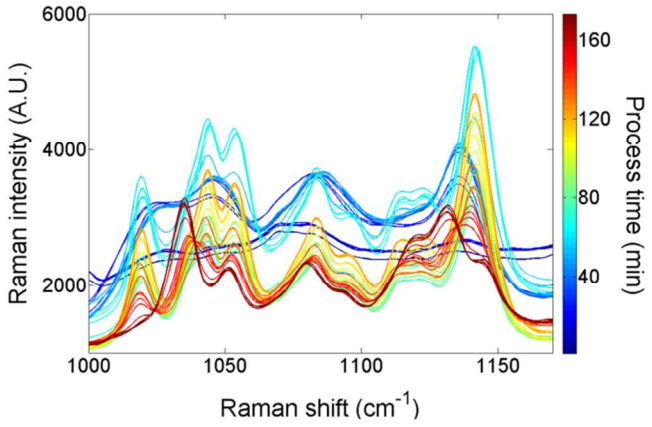

Figure S-1. Raw Raman process spectra of experiment C. Every 4th spectrum of the process is plotted and colored according to process time.

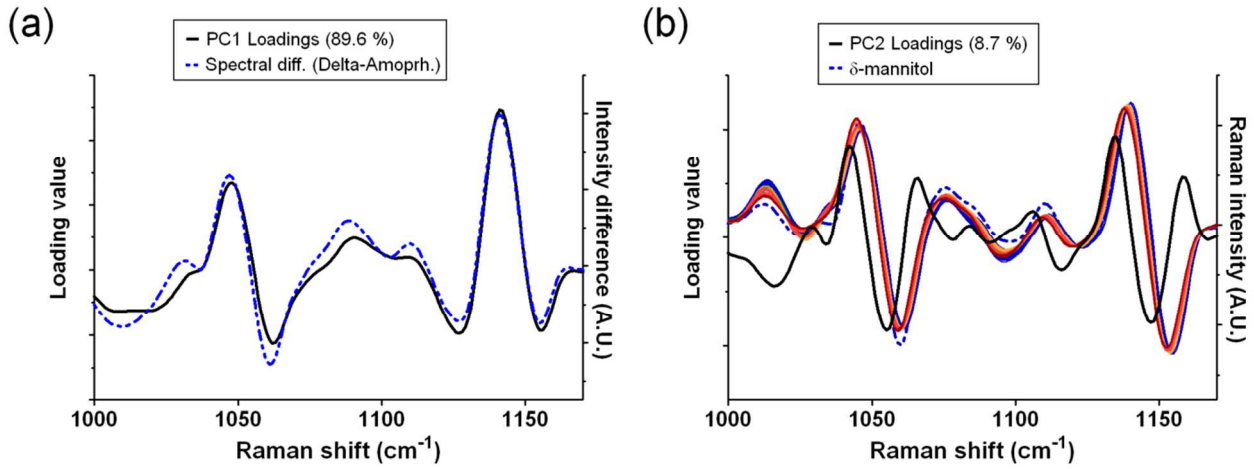

Figure S-2. Interpretation of principal components. PCA of experiment A: Fast cooling with annealing. (a) The loadings of PC1 plotted with differential spectrum of δ- and amorphous form. These graphs show highly similar features and therefore PC1 was interpreted to describe mainly amorphous form crystallization to δ-form. (b) The loadings of PC2 plotted with Raman spectrum of δ-mannitol and process spectra 17-131. These process spectra were inspected as those presented the greatest variation to the PC2 in the score plot (Figure 3A). Process spectra are colored according to measurement temperature which ranged from -50 to +80 °C. Process spectra, that resembles spectrum of δ-mannitol, show no signs of solid-state transformation but are slightly shifted to lower wavenumbers as temperature increases. Therefore PC2 was interpreted to describe temperature associated changes in spectra.

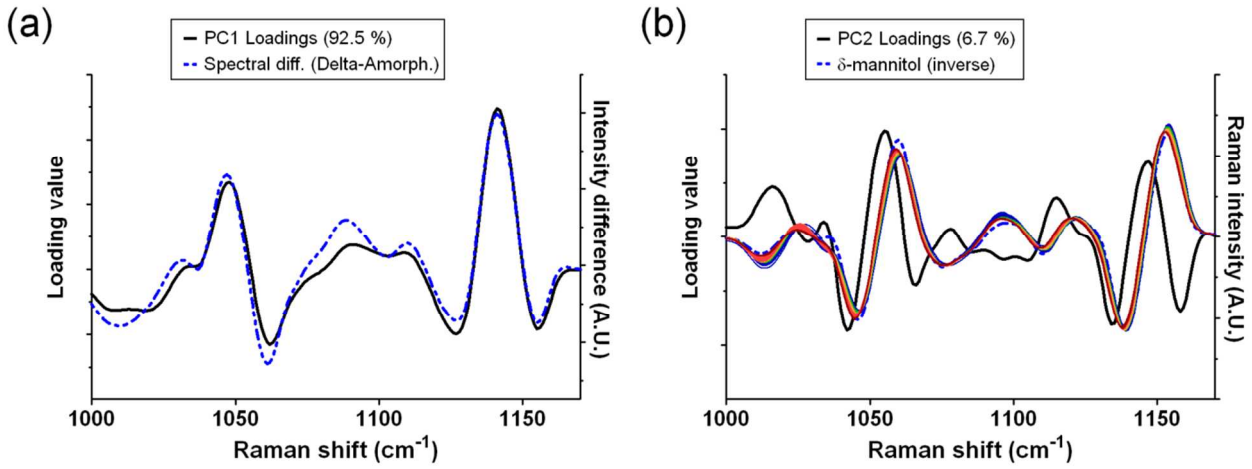

Figure S-3. Interpretation of principal components. PCA of experiment B: Fast cooling without annealing. (a) The loadings of PC1 plotted with differential spectrum of δ- and amorphous form. These graphs show a common uniformity and therefore PC1 was interpreted to describe mainly amorphous form crystallization to δ-form. (b) The loadings of PC2 plotted with inverse Raman spectrum of δ-mannitol and inverse process spectra 17-113. These process spectra were inspected as those presented the greatest variation to PC2 in the score plot (Figure 3B). Inversion of spectra was done to enable direct comparison with the loadings as the shift of the scores occurred in negative direction along PC2. Process spectra are colored according to measurement temperature which ranged from -15 to +80 °C. Process spectra, that resembles spectrum of δ-mannitol, show no signs of solid-state transformation but are slightly shifted to lower wavenumbers as temperature increases. Therefore PC2 was interpreted to describe temperature associated changes in spectra.

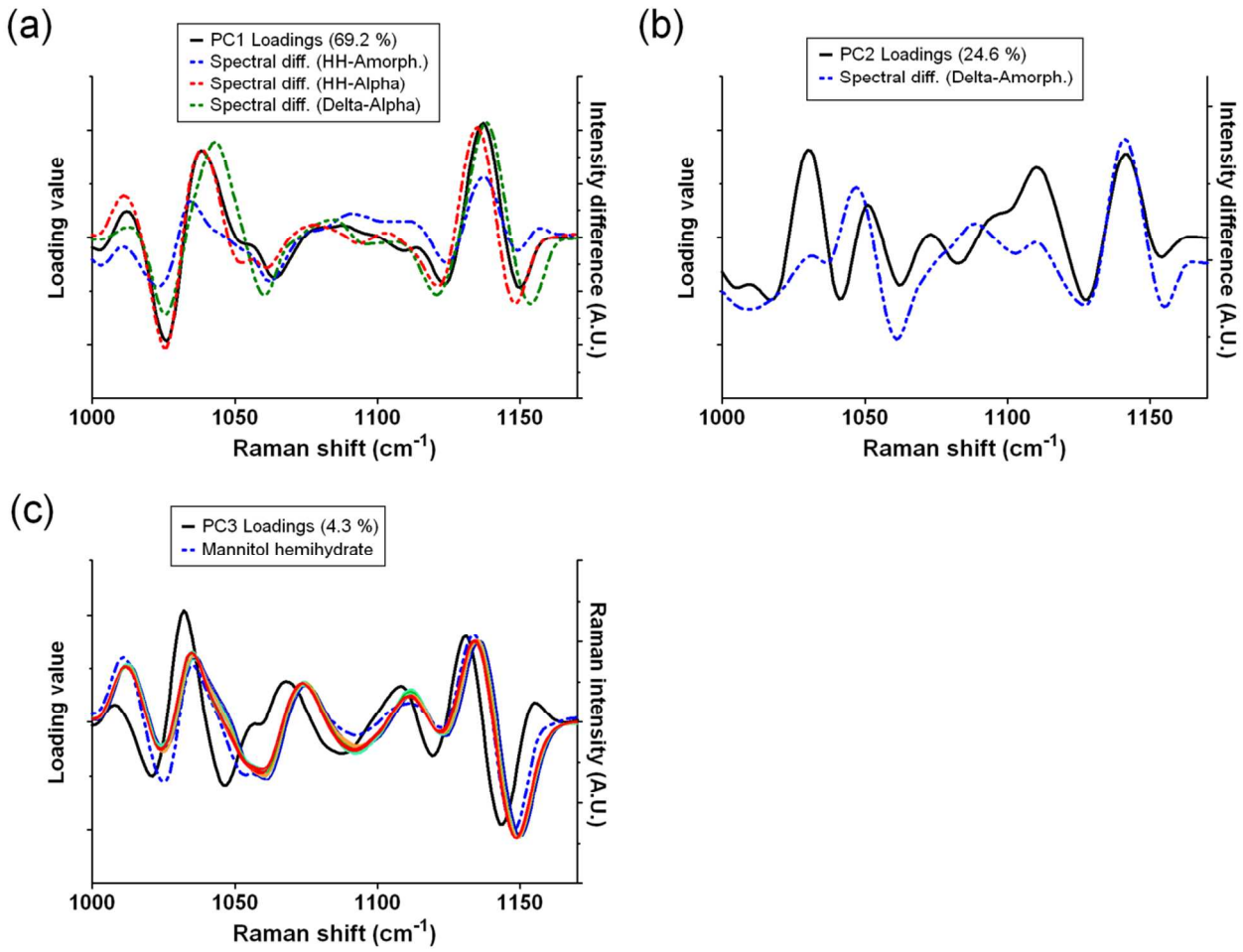

Figure S-4. Interpretation of principal components. PCA of experiment C: Standard cooling with annealing. (a) The loadings of PC1 plotted with differential spectra of hemihydrate and amorphous form (blue), hemihydrate and α-form (red) and δ- and α-form (green). All of these graphs show similar features. As score plot in Figure 3C showed, various transitions occurred along PC1 axis. Therefore PC1 was interpreted to describe various spectral transitions. (b) The loadings of P21 plotted with differential spectrum of δ- and amorphous form. These graphs show some similarities and therefore PC2 was interpreted to describe to some extent amorphous form crystallization to δ-form. (c) The loadings of PC3 plotted with Raman spectrum of mannitol hemihydrate and process spectra 63-139. These process spectra presented the greatest variation to PC3 in the score plot. Process spectra are colored according to measurement temperature which ranged from -50 to +60 °C. Process spectra, that resembles spectrum of mannitol hemihydrate, show no signs of solid-state transformation but are slightly shifted to lower wavenumbers as temperature increases. Therefore PC3 was interpreted to describe temperature associated changes in spectra.

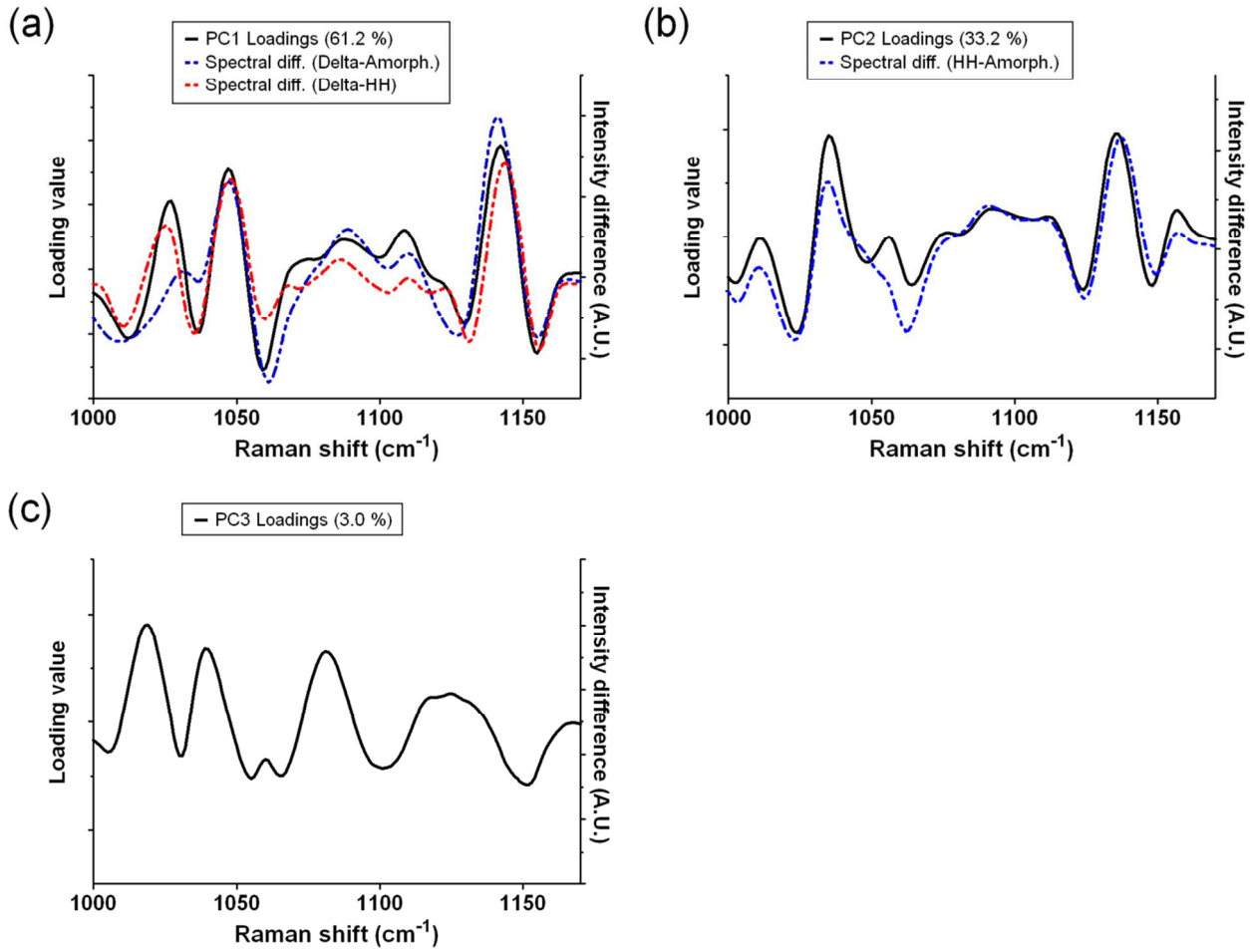

Figure S-5. Interpretation of principal components. PCA of experiment D: Standard cooling without annealing. (a) The loadings of PC1 plotted with differential spectra of δ- and amorphous form (blue) and δ- and hemihydrate form (red). All of these graphs show similar features. Therefore PC1 was interpreted to describe mainly formation of δ-form of mannitol. (b) The loadings of P21 plotted with differential spectrum of hemihydrate and amorphous form. These graphs show some similarities and therefore PC2 was interpreted to describe mainly amorphous form crystallization to mannitol hemihydrate. (c) The loadings of PC3. The origin of this principal component could not be explicitly solved so it was thought to originate from various minor spectral changes.

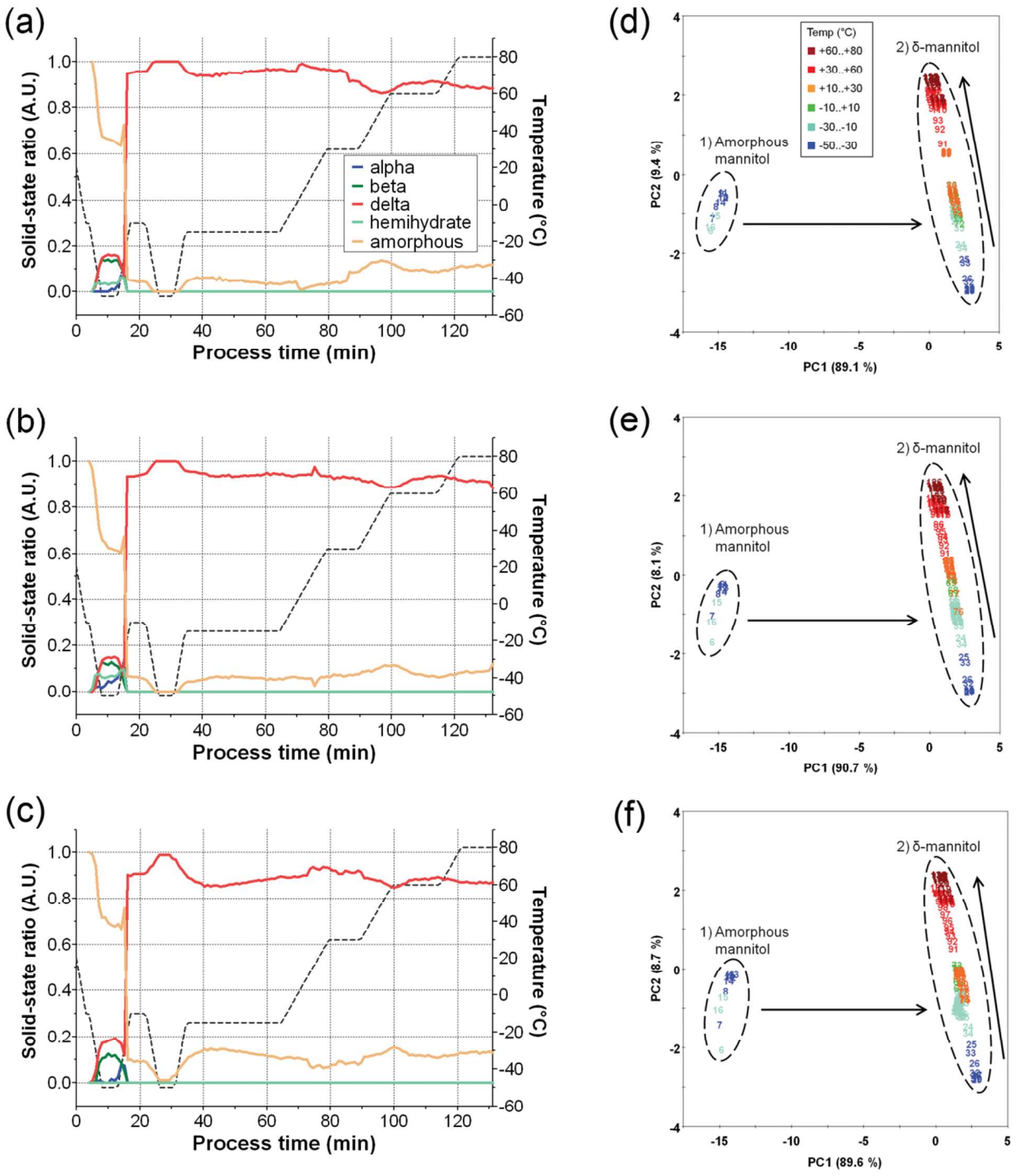

Figure S-6. (a) – (c) CLS plots and (d) – (f) PCA score plots of replicate measurements of experiment A: Fast cooling with annealing.

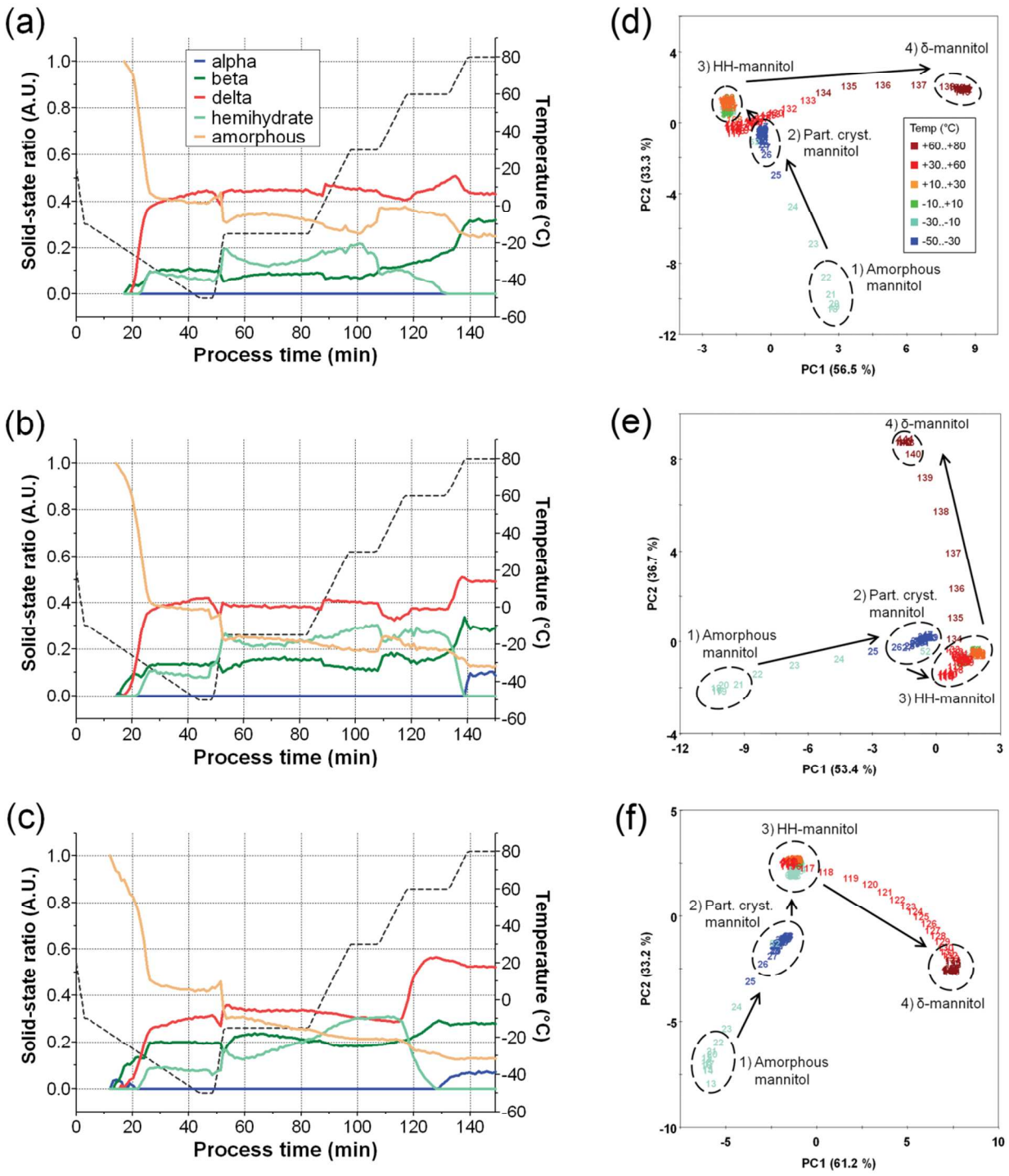

Figure S-7. (a) – (c) CLS plots and (d) – (f) PCA score plots of replicate measurements of experiment D: Standard cooling without annealing.

Table S-2. CLS estimated ratios of mannitol solid-state forms present at the different process phases. Solid-state forms of end-product are also presented from off-line XRPD data.

Experiment	End of primary drying at -15 °C	End of secondary drying at +30 °C	End-product characteristics	
			CLS	XRPD
C Fast cooling with annealing	δ ~ 90 % Amo ~ 10 %	δ ~ 90 % Amo ~ 10 %	δ ~ 90 % Amo ~ 10 %	δ, Amo
B Fast cooling without annealing	δ ~ 90 % Amo ~ 10 %	δ ~ 90 % Amo ~ 10 %	δ ~ 90 % Amo ~ 10 %	δ, β, Amo
C Standard cooling with annealing	β ~ 20 % δ ~ 40 % HH ~ 15 % Amo ~ 25 %	β ~ 15 % δ ~ 40 % HH ~ 25 % Amo ~ 20 %	α ~ 30 % β ~ 45 % δ ~ 10 % Amo ~ 15 %	α, β, δ, Amo
D Standard cooling without annealing	β ~ 20 % δ ~ 35 % HH ~ 20 % Amo ~ 25 %	β ~ 20 % δ ~ 30 % HH ~ 30 % Amo ~ 20 %	α ~ 5 % β ~ 30 % δ ~ 50 % Amo ~ 15 %	α, β, δ, Amo

HH = mannitol hemihydrate

Amo = amorphous mannitol